

Non-unitary neutrino mixing and CP violation in the minimal inverse seesaw model

Michal Malinský,^{1,*} Tommy Ohlsson,^{1,†} Zhi-zhong Xing,^{2,‡} and He Zhang^{1,§}

*¹Department of Theoretical Physics, School of Engineering Sciences,
Royal Institute of Technology (KTH) – AlbaNova University Center,
Roslagstullsbacken 21, 106 91 Stockholm, Sweden*

*²Institute of High Energy Physics and Theoretical Physics Center for Science Facilities,
Chinese Academy of Sciences, P.O. Box 918, Beijing 100049, China*

(Dated: August 30, 2018)

Abstract

We propose a simplified version of the inverse seesaw model, in which only two pairs of the gauge-singlet neutrinos are introduced, to interpret the observed neutrino mass hierarchy and lepton flavor mixing at or below the TeV scale. This “minimal” inverse seesaw scenario (MISS) is technically natural and experimentally testable. In particular, we show that the effective parameters describing the non-unitary neutrino mixing matrix are strongly correlated in the MISS, and thus, their upper bounds can be constrained by current experimental data in a more restrictive way. The Jarlskog invariants of non-unitary CP violation are calculated, and the discovery potential of such new CP-violating effects in the near detector of a neutrino factory is discussed.

*Electronic address: malinsky@kth.se

†Electronic address: tommy@theophys.kth.se

‡Electronic address: xingzz@ihep.ac.cn

§Electronic address: zhanghe@kth.se

I. INTRODUCTION

Among various theoretical attempts, the famous seesaw ideas provide us with a very natural way to understand why the masses of three known neutrinos are so tiny compared to the masses of other Standard Model (SM) fermions [1, 2, 3, 4, 5, 6, 7]. In the canonical type-I seesaw mechanism, in which three right-handed (RH) neutrinos are introduced and lepton number violation is allowed, the effective mass matrix of three light Majorana neutrinos m_ν is dramatically suppressed with respect to the electroweak scale if the RH neutrino mass matrix M_R is located not far away from the typical scale of grand unified theories. As a rough estimate, if light neutrino masses are stabilized around the sub-eV scale and the Dirac mass matrix M_D between left- and right-handed neutrinos is comparable with the mass of the top quark, then $M_R \sim 10^{14}$ GeV is naturally expected. The testability of such conventional seesaw models is therefore questionable. On the other hand, it is difficult to embed RH neutrinos into a theoretical framework at low-energy scales [e.g., the TeV scale to be explored by the Large Hadron Collider (LHC)] in a technically natural way while keeping the left-handed neutrinos to be light enough. For those realistically viable type-I or type-III seesaw models with the TeV-scale RH neutrinos, which could be experimentally accessible at the LHC, fine-tunings of cancellations among the contributions to m_ν from different heavy neutrinos have to be employed. These kinds of structural cancellations are usually attributed to some underlying flavor symmetries [8, 9, 10, 11, 12]. In the type-(I+II) seesaw model, one may also assume the mass term coming from RH neutrinos to be comparable with the one coming from the triplet Higgs, and thus, the light neutrino mass scale is brought down through a significant cancellation between these two mass terms [13]. However, to generate appreciable collider signatures of the heavy seesaw particles at the LHC, such a scheme potentially suffers from dangerous radiative corrections and requires unnatural fine-tuning even at loop level [14].

In our recent work [15], we have pointed out that the above-mentioned drawbacks of most TeV-scale type-I, type-III, and type-(I+II) seesaw models can be circumvented by considering the inverse seesaw model [16]. In the latter framework, additional SM gauge singlets are adhibited together with a small Majorana mass insertion which explicitly breaks the lepton number. The phenomenology of this inverse seesaw mechanism is very rich: on the one hand, non-unitary neutrino mixing and CP violation can naturally show up and

are possible to be tested at the future long-baseline neutrino oscillation experiments; on the other hand, the heavy seesaw particles may result in very attractive signatures of lepton-flavor-violating (LFV) processes at the LHC. Since the heavy singlets possess opposite CP signs and compose the pseudo-Dirac particles in pair, the lepton-number-violating (LNV) processes (such as the like-sign di-lepton events at the LHC) are significantly suppressed and practically invisible.

However, the inverse seesaw scenario with three heavy singlet pairs contains too many free parameters and is not very predictive. To partly avoid this drawback, one may consider a simplified version of the generic inverse seesaw scenario by reducing its number of degrees of freedom. This sound motivation leads us to the minimal inverse seesaw scenario (MISS) at the TeV scale, in which only two pairs of the SM gauge-singlet neutrinos are introduced but the observed neutrino mass hierarchy and lepton flavor mixing can well be interpreted.¹

The purpose of this work is to describe the MISS, which contains only two RH neutrinos (ν_{R1}, ν_{R2}) and two SM gauge singlets (S_1, S_2), and to explore some of its low-energy consequences on neutrino mixing and CP violation. The remainder of our work is organized as follows. In Sec. II, we will introduce the MISS and present some general formulas associated with the non-unitarity of the light neutrino mixing matrix. In Sec. III, we will constrain the parameter space of non-unitarity effects in the MISS by using current experimental data, calculate the Jarlskog invariants of leptonic CP violation, and discuss the discovery potential of such new CP-violating effects in the near detector of a neutrino factory. Finally, a brief summary will be given in Sec. IV.

II. THE MINIMAL INVERSE SEESAW SCENARIO

The MISS is constructed by extending the SM particle content with two RH neutrinos $\nu_R = (\nu_{R1}, \nu_{R2})$ and two left-handed (LH) SM gauge singlets $S = (S_1, S_2)$. The mass part of the neutrino sector Lagrangian is then arranged so that it reads in the flavor basis

$$-\mathcal{L}_m = \overline{\nu}_L M_D \nu_R + \overline{S} M_R \nu_R + \frac{1}{2} \overline{S} \mu S^c + \text{H.c.} , \quad (1)$$

where μ is a complex symmetric 2×2 matrix and M_D and M_R are arbitrary 3×2 and 2×2 matrices, respectively. Without loss of generality, one can always redefine the extra

¹ See also the minimal type-I seesaw [17, 18] and the minimal type-(I+II) seesaw [19].

singlet fields and work in a basis where μ is real and diagonal, namely, $\mu = \text{diag}(\mu_1, \mu_2)$ with $\mu_1 < \mu_2$. In addition to that, M_R can be made Hermitian by a further unitary transformation in the RH neutrino sector. The 7×7 neutrino mass matrix in the basis (ν_L, ν_R^c, S) is then rewritten as

$$M_\nu = \begin{pmatrix} 0 & M_D & 0 \\ M_D^T & 0 & M_R^T \\ 0 & M_R & \mu \end{pmatrix}, \quad (2)$$

which is clearly a symmetric matrix with rank at most 6 [20].

Note that M_R is a SM singlet mass term, and hence, it is not governed by the scale of the $SU(2)_L$ symmetry breaking. In what follows, we will consider a particularly attractive case $M_R > M_D \gg \mu$, with M_R not far above the electroweak scale. In the limit $\mu \rightarrow 0$, the rank of M_ν reduces from 6 to 4, which leaves three light neutrinos massless. In reality, a tiny but non-vanishing μ can be viewed as a slight breaking of a global $U(1)$ symmetry, and thus, it respects the naturalness criterion [21]. In contrast to the original inverse seesaw scenario, the MISS predicts one light neutrino to be exactly massless and brings in several interesting phenomena in neutrino oscillations and LFV processes.

At the leading order in $M_D M_R^{-1}$, the light neutrino mass matrix in the MISS is given by

$$m_\nu \simeq M_D M_R^{-1} \mu (M_R^T)^{-1} M_D^T \equiv F \mu F^T, \quad (3)$$

where $F = M_D M_R^{-1}$ is a 3×2 matrix. For μ around the keV scale, $M_D M_R^{-1} \sim 10^{-2}$ gives rise to the desired sub-eV light neutrino masses. In the limit $\mu \rightarrow 0$, we have $m_\nu = 0$, which corresponds to the lepton number symmetry restoration. The heavy sector consists of a pair of pseudo-Dirac neutrinos $P_j = (S_j, \nu_{Rj})$ [22] with a tiny mass splitting between the relevant CP-conjugated Majorana components of the order of μ .

One can diagonalize m_ν by means of a unitary transformation

$$U^\dagger m_\nu U^* = \bar{m}_\nu = \text{diag}(m_1, m_2, m_3), \quad (4)$$

with m_i (for $i = 1, 2, 3$) denoting the light neutrino masses. We are left with either $m_1 = 0$ (normal mass hierarchy $\Delta m_{31}^2 > 0$, NH) or $m_3 = 0$ (inverted mass hierarchy $\Delta m_{31}^2 < 0$, IH). Note that U itself is not the matrix that governs neutrino oscillations even if we choose a basis where the charged-lepton mass matrix is diagonal.

The LH neutrinos entering the charged-current interactions of the SM are superpositions of the seven mass eigenstates (ν_{mL}, P_m) given at the leading order by

$$\nu_L \simeq N\nu_{mL} + FU_R P_{mL} , \quad (5)$$

where $U_R^\dagger M_R U_R = \text{diag}(m_{P_1}, m_{P_2})$ and $N \simeq (1 - \frac{1}{2}FF^\dagger) U$ [23]. Hence, one can write

$$\mathcal{L}_{CC} = -\frac{g}{\sqrt{2}} W_\mu^- \bar{\ell}_L \gamma^\mu (N\nu_{mL} + FU_R P_{mL}) + \text{H.c.} \quad (6)$$

The mixing between the doublet and singlet components in the charged currents results in several interesting phenomenological consequences:

- The flavor and mass eigenstates of the left-handed neutrinos are connected by a non-unitary flavor mixing matrix N [24]. The magnitudes of non-unitarity effects in different neutrino oscillation channels are predominated by the mass ratios between M_D and M_R , and in principle, their underlying correlations have to be taken into account in analyses of the future experiments.
- The heavy singlets entering the charged currents due to the non-unitarity effects also enter the rare lepton decays, such as $\tau \rightarrow \mu\gamma$ and $\mu \rightarrow e\gamma$. Hence, unlike in the type-I seesaw model, their contributions to the LFV decays are not suppressed by the light neutrino masses [25], but mainly constrained by the ratio $M_D M_R^{-1}$, which in principle admits observing these events in the upcoming LHC experiments. For example, the decays $\ell_\alpha \rightarrow \ell_\beta \gamma$ are mediated by P 's and their branching ratios are given by [26]

$$\text{BR}(\ell_\alpha \rightarrow \ell_\beta \gamma) = \frac{\alpha_W^3 s_W^2 m_{\ell_\alpha}^5}{256\pi^2 M_W^4 \Gamma_\alpha} \left| \sum_{i=1}^2 K_{\alpha i} K_{\beta i}^* I\left(\frac{m_{P_i}}{M_W^2}\right) \right|^2 , \quad (7)$$

where $K = FU_R$, $I(x) = -(2x^3 + 5x^2 - x)/[4(1-x)^3] - 3x^3 \ln x/[2(1-x)^4]$, and Γ_α is the total width of ℓ_α . In the conventional type-I seesaw model (i.e., without unnatural cancellations), one has approximately $KK^\dagger = \mathcal{O}(m_\nu M_R^{-1})$, and therefore, $\text{BR}(\ell_\alpha \rightarrow \ell_\beta \gamma) \propto \mathcal{O}(m_\nu^2)$ indicates a strong suppression of LFV decays. However, in the inverse seesaw model, one can have sizable K without any reference to the tiny neutrino masses, since the two issues are essentially decoupled. Thus, appreciable LFV rates could be obtained even for strictly massless light neutrinos [27].

- If the masses of the heavy singlets P_m do not fall far beyond the electroweak scale, in the MISS, as in the type-I seesaw model, one can expect an on-shell production of P

at the LHC via the gauge boson exchange diagrams. The most distinctive signature would be the observation of LFV processes involving three charged-leptons in the final state [28].

In comparison to the generic inverse seesaw scenario, the MISS is certainly more restrictive and predictive because of its much fewer free parameters and underlying correlations among physical observables, which could be well tested at a future neutrino factory. In the remaining part of this work, we will discuss the phenomenological consequences mentioned above in more detail and, in particular, concentrate on the possible non-unitary CP-violating effects in neutrino oscillations.

III. NON-UNITARITY EFFECTS

A. Constraints on non-unitarity parameters

As we have already mentioned, light neutrino mass eigenstates are connected to their flavor eigenstates by a non-unitary mixing matrix N . In terms of the parametrization advocated in Ref. [29], the non-unitary leptonic mixing is written as $N = (1 - \eta)U$ where the relevant Hermitian matrix η is given by $\eta \simeq \frac{1}{2}FF^\dagger$ and the unitary matrix U can be parametrized in the standard form

$$U = \begin{pmatrix} c_{12}c_{13} & s_{12}c_{13} & s_{13}e^{-i\delta} \\ -s_{12}c_{23} - c_{12}s_{23}s_{13}e^{i\delta} & c_{12}c_{23} - s_{12}s_{23}s_{13}e^{i\delta} & s_{23}c_{13} \\ s_{12}s_{23} - c_{12}c_{23}s_{13}e^{i\delta} & -c_{12}s_{23} - s_{12}c_{23}s_{13}e^{i\delta} & c_{23}c_{13} \end{pmatrix} \begin{pmatrix} 1 \\ e^{i\rho} \\ 1 \end{pmatrix}, \quad (8)$$

provided $c_{ij} \equiv \cos \theta_{ij}$ and $s_{ij} \equiv \sin \theta_{ij}$ (for $ij = 12, 13, 23$). Since one light neutrino mass is vanishing in the MISS, we have only one Majorana phase. The current experimental bounds on η are rather stringent, implying that one can approximate θ_{ij} 's by the values of the mixing angles obtained from the neutrino oscillations. Present data on atmospheric, solar, and reactor neutrinos yield two neutrino mass-squared differences $\Delta m_{21}^2 \simeq 7.65 \times 10^{-5}$ eV and $|\Delta m_{31}^2| \simeq 2.40 \times 10^{-3}$ eV, together with three neutrino mixings $\sin^2 \theta_{12} \simeq 0.304$, $\sin^2 \theta_{23} \simeq 0.50$, and $\sin^2 \theta_{13} \simeq 0.01$ [30]. There is no hint on the CP-violating phases, and thus, we take $\theta_{13} < 10^\circ$ and leave δ as a free parameter in the following calculations. As for the non-unitarity parameters, $|\eta_{\alpha\beta}|$ are constrained mainly from universality tests of weak

interactions, rare leptonic decays, invisible width of the Z -boson and neutrino oscillation data. The present bounds on $|\eta_{\alpha\beta}|$ (at the 90 % C.L.) are [31]:

$$|\eta| \equiv (|\eta_{\alpha\beta}|) < \begin{pmatrix} 2.0 \times 10^{-3} & 6.0 \times 10^{-5} & 1.6 \times 10^{-3} \\ \sim & 8.0 \times 10^{-4} & 1.1 \times 10^{-3} \\ \sim & \sim & 2.7 \times 10^{-3} \end{pmatrix}. \quad (9)$$

In order to study the connections among physical parameters in the MISS, we adopt the parametrization of F from the work in Ref. [32], namely

$$F = U\sqrt{\bar{m}_\nu}R\sqrt{\mu^{-1}}, \quad (10)$$

where

$$R = \begin{pmatrix} 0 & 0 \\ \cos z & -\sin z \\ \sin z & \cos z \end{pmatrix}, \quad (11)$$

for the NH case, and

$$R = \begin{pmatrix} \cos z & -\sin z \\ \sin z & \cos z \\ 0 & 0 \end{pmatrix}, \quad (12)$$

for the IH case. Here $z = \alpha + i\beta$ is an arbitrary complex number with both α and β being real. For sake of simplicity, in what follows we will use the parameters $r \equiv \mu_1/\mu_2$ and $\epsilon \equiv \sqrt[4]{\Delta m_{21}^2/|\Delta m_{31}^2|} \simeq 0.42$. In the NH case, we obtain

$$F = \sqrt{\frac{m_3}{\mu_2}} \begin{pmatrix} 0 & 0 \\ \frac{1}{\sqrt{r}} s_{23} s_z & s_{23} c_z \\ \frac{1}{\sqrt{r}} c_{23} s_z & c_{23} c_z \end{pmatrix} + \mathcal{O}(\epsilon), \quad (13)$$

which yields

$$\eta \simeq \frac{1}{2} \frac{m_3}{\mu_2} \frac{r|c_z|^2 + |s_z|^2}{2r} \begin{pmatrix} 0 & 0 & 0 \\ 0 & s_{23}^2 & s_{23} c_{23} \\ 0 & s_{23} c_{23} & c_{23}^2 \end{pmatrix}. \quad (14)$$

Thus, the only non-negligible off-diagonal entry is $\eta_{\mu\tau}$, and we have the relation $|\eta_{\mu\mu}| \simeq |\eta_{\mu\tau}| \simeq |\eta_{\tau\tau}|$ because, to a good approximation, $\theta_{23} \simeq 45^\circ$. Similarly, in the IH case, we obtain

$$F = \sqrt{\frac{m_1}{\mu_2}} \begin{pmatrix} \frac{1}{\sqrt{r}}A & B \\ -\frac{1}{\sqrt{r}}c_{23}X & c_{23}Y \\ \frac{1}{\sqrt{r}}s_{23}X & -s_{23}Y \end{pmatrix} + \mathcal{O}(\epsilon^2), \quad (15)$$

which translates into

$$\eta \simeq \frac{1}{2} \frac{m_1}{\mu_2} \begin{pmatrix} \frac{1}{r}A^2 + B^2 & -c_{23} \left(\frac{1}{r}AX^* - BY^* \right) & s_{23} \left(\frac{1}{r}AX^* - BY^* \right) \\ \sim & c_{23}^2 \left(\frac{1}{r}|X|^2 + |Y|^2 \right) & -s_{23}c_{23} \left(\frac{1}{r}|X|^2 + |Y|^2 \right) \\ \sim & \sim & s_{23}^2 \left(\frac{1}{r}|X|^2 + |Y|^2 \right) \end{pmatrix}, \quad (16)$$

where $A = c_{12}c_z + e^{i\rho}s_{12}s_z$, $B = -c_{12}s_z + e^{i\rho}s_{12}c_z$, $X = s_{12}c_z - e^{i\rho}c_{12}s_z$, and $Y = s_{12}s_z + e^{i\rho}c_{12}c_z$. Hence, in both cases, the approximately maximal leptonic 23 mixing implies $|\eta_{\mu\mu}| \simeq |\eta_{\mu\tau}| \simeq |\eta_{\tau\tau}|$ and $|\eta_{e\mu}| \simeq |\eta_{e\tau}|$.

The allowed regions of non-unitarity parameters are illustrated in Figs. 1 and 2. In total, we have eleven parameters out of which seven ($\mu_1, \mu_2, \alpha, \beta, \rho, \delta, \theta_{13}$) are essentially free while the remaining four ($\theta_{12}, \theta_{23}, \Delta m_{21}^2, \Delta m_{31}^2$) are quantities fixed by their best-fit values. In our numerical analysis, we randomly generate points in the seven-dimensional parameter space. The points that are within the 90 % C.L. upper bounds on the non-unitarity parameters $\eta_{\alpha\beta}$ are plotted in the figures, where we do not resort to the approximate Eqs. (13)-(16) but rather utilize the precise Eq. (10). As a result, 10^4 points build up each plot. Using Eq. (3), one can easily estimate that $\mu_2 \gg m_i$ should be ensured if there is no strong structural cancellations in F . Hence, in our numerical calculations, we set $|\Delta m_{31}^2|/\mu_2 < 0.01$ as a prior in order to avoid unnatural fine-tuning among model parameters.

It is important to make clear that the decrease of the point-density towards smaller values of $|\eta_{\alpha\beta}|$ is a mere numerical artifact, since these regions correspond to a physically not very interesting situation, and hence, it does not make sense to scan over such areas thoroughly. On the other hand, the density reduction observed in the opposite (i.e., growing $|\eta_{\alpha\beta}|$) directions, c.f., the two upper plots in Fig. 1, provides a true physical information and all the following statements are based on such kind of physically relevant features.

In Fig. 1, we present the allowed regions for the absolute values of the relevant non-unitarity parameters. The upper-left plot shows the correlation between $|\eta_{\mu\mu}|$ and $|\eta_{\mu\tau}|$,

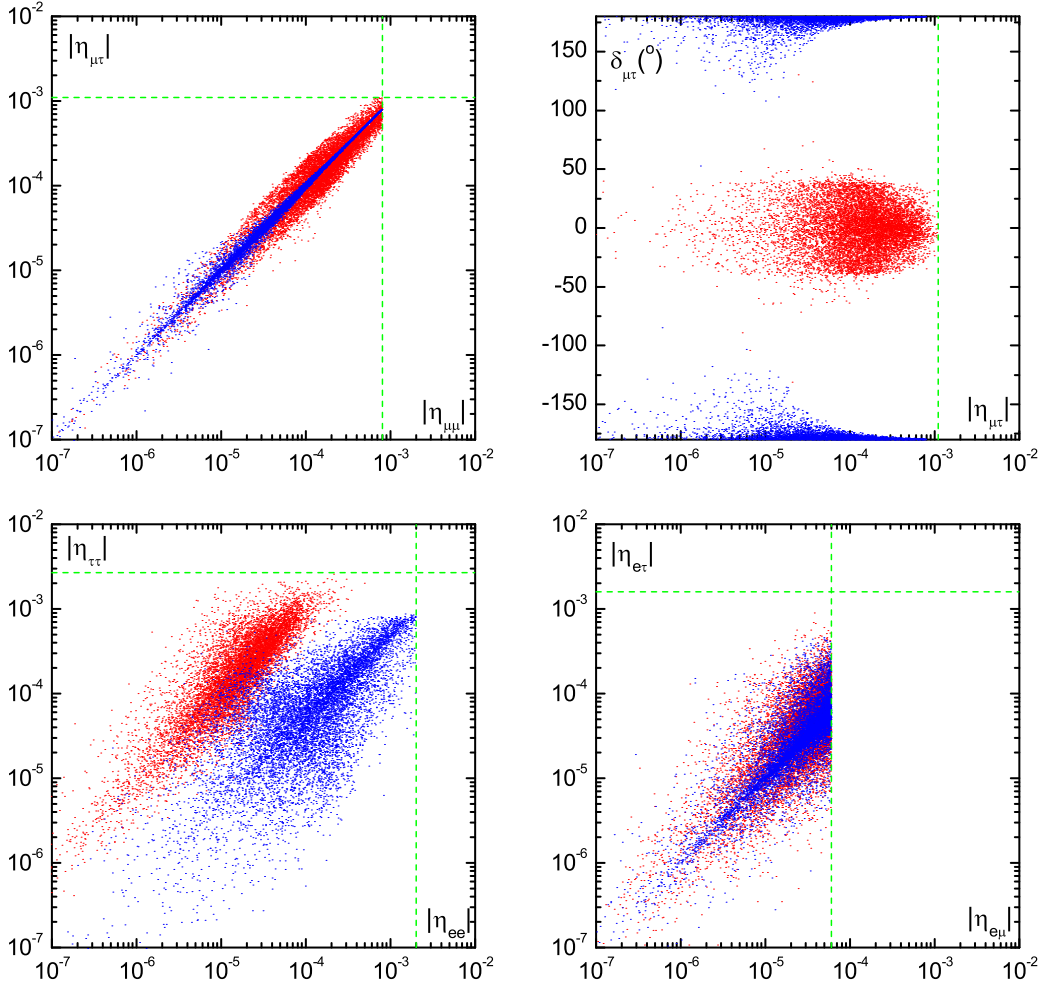


FIG. 1: Correlations among various parameters governing the non-unitarity effects in the MISS. Red points denote the normal neutrino mass hierarchy, while blue points correspond to the case of the inverted mass hierarchy. Generic experimental constraints are indicated by the green dashed lines (and, for simplicity, any would-be correlations in their determination have been neglected).

which is stronger in the IH case than in the NH case. This is expected, since the analytical approximation in the IH case is better than that in the NH case. The upper-right plot shows the CP-violating phase $\delta_{\mu\tau}$ of the parameter $\eta_{\mu\tau}$, which is centered around 0 in the NH case and around $\pm 180^\circ$ in the IH case, in agreement with Eqs. (14) and (16). Thus, in both cases, it is hard to achieve a sizable $|\eta_{\mu\tau}|$ and maximal CP-violating effects simultaneously. The bounds on the other η parameters are shown in the plots in the second row of Fig. 1.

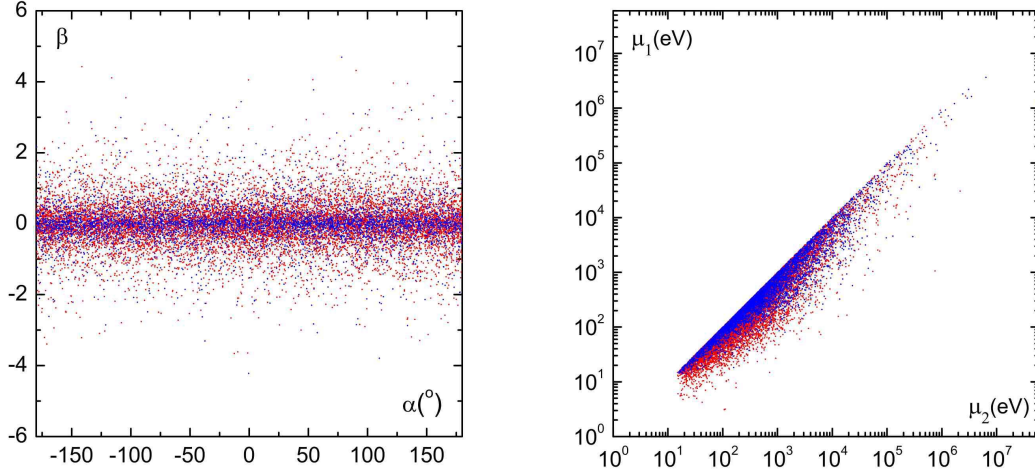


FIG. 2: Constraints on the underlying model parameters. As before, red and blue points denote the normal and inverted neutrino mass hierarchies, respectively. As described in the text, the $|\beta| \gg 1$ and $\mu_2 \rightarrow 0$ regions correspond to a fine-tuning, which we wish to avoid, and thus, the scanning granularity is large. Moreover, $\mu_1 \rightarrow 0$ leads to a further reduction of the rank of m_ν , and hence, it is also disfavored.

One can observe that $|\eta_{ee}|$ is mainly constrained in the NH case, while $|\eta_{\tau\tau}|$ is restricted in the IH case. The allowed region for $|\eta_{e\tau}|$ is limited in both NH and IH cases, and there is no upgraded bound on $|\eta_{e\mu}|$. Note that, in the NH case, the leading order formulae (13) and (14) do not provide as good approximation of the precise results as do the Eqs. (15) and (16) in the IH case, because the relevant effective expansion parameters (i.e., ε^2 in the latter whilst only ε in the former case) are not the same. This also imprints into the different widths of the red and blue bands in Fig. 1.

The allowed regions for μ_i and z are shown in Fig. 2. There is no strong constraint on α . However, β is bounded, since a larger β corresponds to a more severe fine-tuning of the model parameters. As for the μ_i parameters, there are no generic upper bounds one should impose; however, smaller values of μ_i correspond to a stronger fine-tuning entangled in F .

Finally, let us summarize the upgraded bounds on the non-unitarity parameters we have obtained in the MISS under consideration: $|\eta_{ee}| \lesssim 5.0 \times 10^{-4}$, $|\eta_{e\tau}| \lesssim 8.9 \times 10^{-4}$ in the NH case, and $|\eta_{e\tau}| \lesssim 4.6 \times 10^{-4}$, $|\eta_{\mu\tau}| \lesssim 7.9 \times 10^{-4}$, $|\eta_{\tau\tau}| \lesssim 8.8 \times 10^{-4}$ in the IH case. They

could be helpful when building a specific and realistic model based on the MISS.

B. Jarlskog invariants

In general, there are nine independent rephasing-invariant quantities that one can build at the quartic level out of the entries of a generic 3×3 lepton mixing matrix V [33],

$$J_{\alpha\beta}^{ij} = \text{Im}(V_{\alpha i} V_{\beta j} V_{\alpha j}^* V_{\beta i}^*) , \quad (17)$$

where the indices $\alpha \neq \beta$ run over $e\mu$, $\mu\tau$ and τe , while $i \neq j$ can be 12, 23 and 31. Note that all nine J_{ab}^{ij} 's coincide if V is a unitary matrix, since all six unitarity triangles, despite their different shapes, span the same area [34, 35]. However, if non-unitarity effects (like those studied in this work, i.e., $V = N$) are present, this is no longer the case and one can expect deviations from such a simple picture driven by the relevant non-unitarity parameters (denoted by $\eta_{\alpha\beta}$ in the current study). In such a case, it is instructive to know which configuration of $\alpha \neq \beta$ and $i \neq j$ is most affected for a specific non-unitarity pattern. In particular, to leading order in $\eta_{\alpha\beta}$, one can write

$$J_{\alpha\beta}^{ij} \simeq J + \Delta J_{\alpha\beta}^{ij} , \quad (18)$$

where $J = c_{12}c_{13}^2c_{23}s_{12}s_{13}s_{23}\sin\delta$ governs the CP-violating effects in the unitary limit. The second term in Eq. (18) depends on the off-diagonal (generally complex) η 's, and hence, it does not necessarily vanish in the limit $\theta_{13} \rightarrow 0$ and might even dominate the CP-violating effects. The complete expressions for $\Delta J_{\alpha\beta}^{ij}$ are listed in Appendix A. Focusing on the dominant off-diagonal entry $|\eta_{\mu\tau}|$, c.f. Fig. 1, the following two contributions survive for $\eta_{e\mu} \rightarrow 0$ and $\theta_{13} \rightarrow 0$:

$$\Delta J_{\mu\tau}^{23} = -|\eta_{\mu\tau}| \sin\delta_{\mu\tau} \sin 2\theta_{23} \cos^2\theta_{12} - |\eta_{e\tau}| s_{12}c_{12}s_{23}c_{23}^2 \sin\delta_{e\tau} , \quad (19)$$

$$\Delta J_{\mu\tau}^{31} = |\eta_{\mu\tau}| \sin\delta_{\mu\tau} \sin 2\theta_{23} \sin^2\theta_{12} - |\eta_{e\tau}| s_{12}c_{12}s_{23}c_{23}^2 \sin\delta_{e\tau} , \quad (20)$$

provided $\eta_{\alpha\beta} = |\eta_{\alpha\beta}|e^{i\delta_{\alpha\beta}}$. Even beyond the simple limit above, one can observe another interesting feature:

$$J_{e\mu}^{23} = J_{e\mu}^{31} = J_{\tau e}^{23} = J_{\tau e}^{31} , \quad (21)$$

where all the small parameters ($\eta_{\alpha\beta}$ and s_{13}) have been kept at linear order. However, these relations are mere reflections of the smallness of the mixing angle θ_{13} .

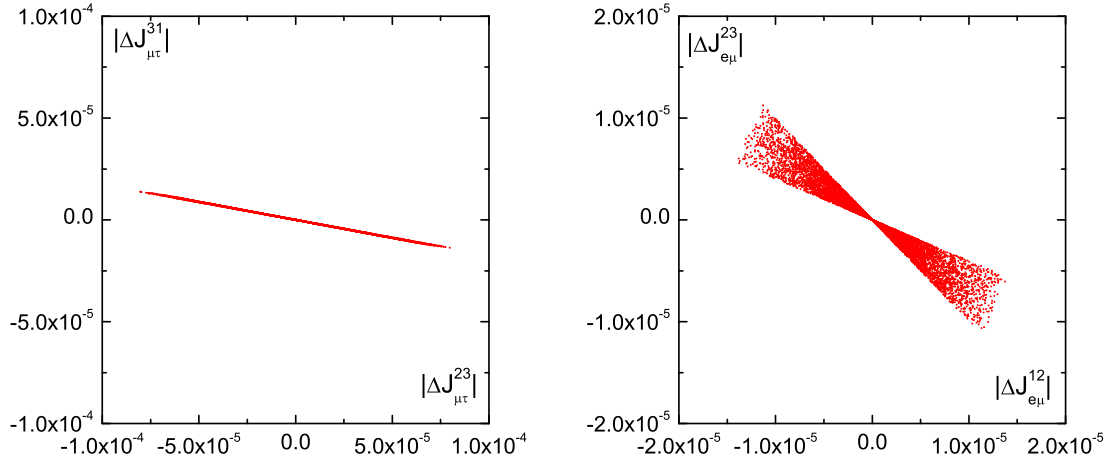


FIG. 3: Constraints on the Jarlskog invariants. Here, only the NH case is considered, since the CP-violating effects due to the non-unitarity parameters are small in the IH case. It is so partly due to the smallness of $\eta_{e\tau}$ and also because of the preferred value of the $\delta_{\mu\tau}$ phase, c.f. Fig. 1.

In Fig. 3, we illustrate the correlations between Jarlskog invariants in the NH case. As we expect, they are linearly dependent, and the spread (i.e., the finite width of the allowed strips) is due to higher-order corrections. Although the magnitude of $\Delta J_{\mu\tau}^{31}$ does not seem to be comparable to that of J , we will show later that the CP-violating effects induced by the phases of non-unitarity parameters can be quite significant, since they are not suppressed by the small neutrino mass-squared difference Δm_{21}^2 . For the IH case, according to Eq. (16), $\eta_{e\mu} \sim \eta_{e\tau}$ are small quantities, and the phase of $\eta_{\mu\tau}$ is close to π , c.f. Fig. 1. Hence, there is no observable CP-violating effect coming from the non-unitarity parameters in the IH case.

C. Sensitivity search at a neutrino factory

For a non-unitary lepton flavor mixing matrix N , the vacuum neutrino oscillation transition probability $P_{\alpha\beta}$ can be written as [36]

$$P_{\alpha\beta} = \sum_{i,j} \mathcal{F}_{\alpha\beta}^i \mathcal{F}_{\alpha\beta}^{j*} - 4 \sum_{i>j} \text{Re}(\mathcal{F}_{\alpha\beta}^i \mathcal{F}_{\alpha\beta}^{j*}) \sin^2 \frac{\Delta m_{ij}^2 L}{4E} + 2 \sum_{i>j} \text{Im}(\mathcal{F}_{\alpha\beta}^i \mathcal{F}_{\alpha\beta}^{j*}) \sin \frac{\Delta m_{ij}^2 L}{2E}, \quad (22)$$

where $\Delta m_{ij}^2 \equiv m_i^2 - m_j^2$ are the neutrino mass-squared differences and \mathcal{F}^i are defined by

$$\mathcal{F}_{\alpha\beta}^i \equiv \sum_{\gamma,\rho} (R^*)_{\alpha\gamma} (R^*)_{\rho\beta}^{-1} U_{\gamma i}^* U_{\rho i} \quad (23)$$

with the normalized non-unitary factor

$$R_{\alpha\beta} \equiv \frac{(1 - \eta)_{\alpha\beta}}{[(1 - \eta)(1 - \eta^\dagger)]_{\alpha\alpha}}. \quad (24)$$

If Earth matter effects are taken into account, then one can replace the vacuum quantities U and m_i by their effective matter counterparts, see e.g. Ref. [37].

As mentioned in the literature [38, 39, 40, 41, 42, 43], the $\nu_\mu \rightarrow \nu_\tau$ channel together with a near detector located at a short distance provides the most favorable setup to constrain the non-unitarity effects.² In this respect, we consider the transition probability $P_{\mu\tau}$ for a neutrino factory with a sufficiently short baseline length L . We neglect the tiny matter effects and small contributions of θ_{13} and Δm_{21}^2 . Then, $P_{\mu\tau}$ reads [38]

$$P_{\mu\tau} \simeq 4s_{23}^2 c_{23}^2 \sin^2 \left(\frac{\Delta m_{31}^2 L}{4E} \right) - 4|\eta_{\mu\tau}| \sin \delta_{\mu\tau} s_{23} c_{23} \sin \left(\frac{\Delta m_{31}^2 L}{2E} \right) + 4|\eta_{\mu\tau}|^2, \quad (25)$$

where E is the neutrino beam energy and the second term is CP-odd due to the phase $\delta_{\mu\tau}$, and hence, distinctive CP-violating effects can appear in neutrino oscillations [29, 46]. The last term in Eq. (25) plays the dominant role at ‘zero’ distance, as it does not depend on L .

Note that the shape of the CP-odd term is justified by the structure of the relevant Jarlskog invariants derived in Sec. IIIB. Indeed, the $\text{Im}(\mathcal{F}_{\alpha\beta}^i \mathcal{F}_{\alpha\beta}^{j*})$ factors in Eq. (22) correspond to $-J_{\alpha\beta}^{ij}$ [apart from the irrelevant real rescaling of J due to the denominator in Eq. (24)]. This means that the sum over $i > j$ in the last term of Eq. (22) is proportional to $J_{\mu\tau}^{31} - J_{\mu\tau}^{23} = |\eta_{\mu\tau}| \sin \delta_{\mu\tau} \sin 2\theta_{23}$ provided $\Delta m_{31}^2 \simeq -\Delta m_{23}^2$.

In order to show the feasibility of observing such a signal in the future long-baseline neutrino oscillation experiments, we consider a typical neutrino factory setting with an OPERA-like near detector with fiducial mass of 5 kt. We assume a setup with approximately 10^{21} useful muon decays and five years of neutrino running and another five years of anti-neutrino running. We make use of the GLOBES package [47, 48] with a slight modification of the template Abstract Experiment Definition Language (AEDL) file for the neutrino

² An alternative study for the disappearance channel $\nu_\mu \rightarrow \nu_\mu$ together with a far detector located at 7500 km has been performed in Refs. [44, 45]. In particular, a sensitivity of $\mathcal{O}(10^{-4})$ could be achieved due to matter effects, for which the neutrino oscillation probability is only linearly suppressed in $\eta_{\mu\tau}$.

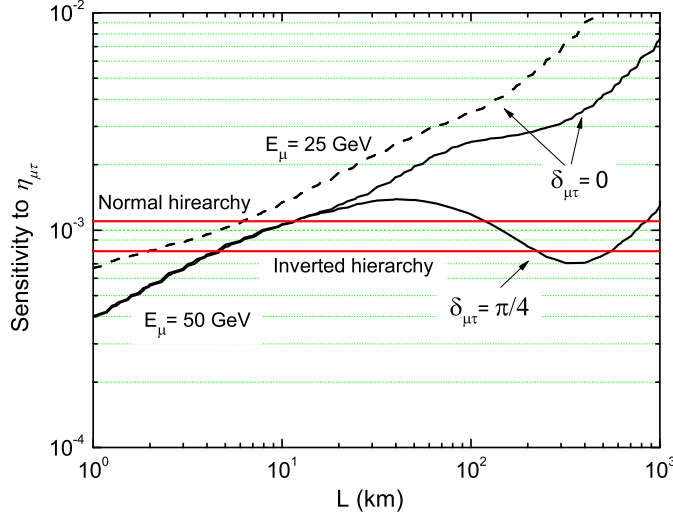


FIG. 4: Sensitivity limits at 90 % C.L. on the non-unitarity parameter $\eta_{\mu\tau}$ as a function of the baseline length L . Solid curves denote the parent muon energy $E_\mu = 50$ GeV with CP phases being labeled in the figure, while the dashed curve corresponds to $E_\mu = 25$ GeV and $\delta_{\mu\tau} = 0$. The bounds on $|\eta_{\mu\tau}|$ in the MISS for the NH and IH cases are also shown by red lines.

factory experiments [49, 50]. In Fig. 4, we display the sensitivity to $\eta_{\mu\tau}$ as a function of the baseline length L for the near detector. One can observe that such a setup provides indeed an excellent probe for this type of non-unitarity effects. An interesting feature, which appears if $\delta_{\mu\tau}$ is sizeable, is that the sensitivity of the near detector will be improved around the baseline length $L \sim 300$ km. This sensitivity enhancement could mainly be regarded as a compromise between new physics effects and the standard neutrino oscillation behavior. At a very short distance, the transition probability $P_{\mu\tau}$ is determined by the last term of Eq. (25), whereas with increasing L , the second term gradually dominates the flavor transitions. Thus, a distance $L \lesssim 500$ km (i.e., the CERN-Fréjus distance) would be favorable for the near detector.

IV. SUMMARY

We have proposed the MISS — an economical low-scale seesaw scenario with minimal particle content in the framework of the inverse seesaw model. Compared to the generic

inverse seesaw mechanism, only two pairs of SM gauge singlets are introduced into the MISS, which gives rise to strong correlations among the non-unitarity parameters. Since one light neutrino has to be massless in this scenario, we have discussed the experimental constraints on these non-unitarity parameters in both NH and IH cases. In view of our numerical and analytical results, the only possibly sizable and phenomenologically interesting non-unitarity parameter is $\eta_{\mu\tau}$, and the current upper bound on $|\eta_{\mu\tau}|$ is improved from 1.1×10^{-3} to 7.9×10^{-4} in the IH case. The Jarlskog invariants in the presence of non-unitary neutrino mixing have been calculated. The relative CP-violating phase of $\eta_{\mu\tau}$ is well constrained by the structure of the MISS, and there are essentially no observable CP-violating effects induced by $\delta_{\mu\tau}$ in the IH case. We have also shown that the CP-violating effects emerging in the MISS can be well tested at a future neutrino factory with an OPERA-like near detector at a distance less than a few hundred kilometers. The possible collider signatures at the LHC and the LFV processes are also promising. However, a detailed analysis exceeds the scope of the current work, and hence, it will be elaborated on elsewhere.

Finally, we would like to stress that the MISS is motivated not only by its simplicity and predictivity, but it can in particular be viewed as a limit of the “standard” ISS setting when the heaviest pseudo-Dirac neutrino essentially decouples. This is the kind of behavior one would expect in grand unified models where a hierarchy in the RH sector is often natural because of the link of the RH-triplet Yukawa couplings to the other parts of the Yukawa sector.³ Alternatively, it is often realized in certain classes of flavor symmetric models in which the RH neutrinos are assigned to some two-dimensional representations of the flavor group, i.e., the smallest group containing one-, two-, and three-dimensional representations of the symmetric permutation group S_4 [53]. One can also adopt a variant of the several strategies proposed to govern the flavor structure of the original inverse seesaw framework, in particular, to accommodate the tri-bimaximal mixing pattern, see e.g. Ref. [54] and references therein. However, a thorough implementation of a flavor symmetry in the given context is beyond the scope of the current work, and will not be further discussed here.

³ In this respect, it is worth noting that the smallness of the RH neutrino mass scale does not in general obstacle the grand-unified constructions, see for instance Refs. [51, 52] and references therein.

Acknowledgments

We wish to thank Mattias Blennow and Enrique Fernández-Martínez for helpful discussions. We acknowledge the hospitality and support from the NORDITA scientific program “Astroparticle Physics — A Pathfinder to New Physics”, March 30 - April 30, 2009 during which most of this study was performed. This work was supported by the Royal Swedish Academy of Sciences (KVA) [T.O.], the Göran Gustafsson Foundation [H.Z.], the Royal Institute of Technology (KTH), contract no. SII-56510 [M.M.], the Swedish Research Council (Vetenskapsrådet), contract no. 621-2008-4210 [T.O.], and the National Natural Science Foundation of China under grant nos. 10425522 and 10875131 [Z.Z.X.].

APPENDIX A: CALCULATION OF JARLSKOG INVARIANTS

The Jarlskog invariants for a non-unitary lepton flavor mixing matrix N are defined by

$$J_{\alpha\beta}^{ij} = \text{Im}(N_{\alpha i} N_{\beta j} N_{\alpha j}^* N_{\beta i}^*) , \quad (\text{A1})$$

provided $N = (1-\eta)U$, where U and η are 3×3 unitary and Hermitian matrices, respectively. The stringent experimental constraints on the deviation of N from U allow one to perform an expansion of Eq. (A1) in powers of the small parameters $\eta_{\alpha\beta}$ and θ_{13} . Up to the second order in $\eta_{\alpha\beta}$ and s_{13} , one has $J_{\alpha\beta}^{ij} \simeq J + \Delta J_{\alpha\beta}^{ij}$, where $J = c_{12}c_{13}^2c_{23}s_{12}s_{13}s_{23}\sin\delta$ and

$$\begin{aligned} \Delta J_{\alpha\beta}^{ij} = & - \sum_{\gamma} \text{Im} \left(\eta_{\alpha\gamma} U_{\gamma i} U_{\beta j} U_{\alpha j}^* U_{\beta i}^* + \eta_{\beta\gamma} U_{\alpha i} U_{\gamma j} U_{\alpha j}^* U_{\beta i}^* \right. \\ & \left. + \eta_{\alpha\gamma}^* U_{\alpha i} U_{\beta j} U_{\gamma j}^* U_{\beta i}^* + \eta_{\beta\gamma}^* U_{\alpha i} U_{\beta j} U_{\alpha j}^* U_{\gamma i}^* \right) . \end{aligned} \quad (\text{A2})$$

In the parametrization (8), the nine relevant Jarlskog invariants read:

$$\Delta J_{e\mu}^{12} = -|\eta_{e\mu}|s_{12}c_{12}c_{23}(1+c_{23}^2)\sin\delta_{e\mu} + |\eta_{e\tau}|s_{12}c_{12}s_{23}c_{23}^2\sin\delta_{e\tau} , \quad (\text{A3})$$

$$\Delta J_{e\mu}^{23} = |\eta_{e\mu}|s_{12}c_{12}s_{23}^2c_{23}\sin\delta_{e\mu} + |\eta_{e\tau}|s_{12}c_{12}s_{23}c_{23}^2\sin\delta_{e\tau} , \quad (\text{A4})$$

$$\Delta J_{\mu\tau}^{23} = -\Delta J_{e\mu}^{23} - 2|\eta_{\mu\tau}|c_{12}^2s_{23}c_{23}\sin\delta_{\mu\tau} , \quad (\text{A5})$$

$$\Delta J_{\mu\tau}^{31} = -\Delta J_{e\mu}^{23} + 2|\eta_{\mu\tau}|s_{12}^2s_{23}c_{23}\sin\delta_{\mu\tau} , \quad (\text{A6})$$

$$\Delta J_{\tau e}^{12} = |\eta_{e\mu}|s_{12}c_{12}s_{23}^2c_{23}\sin\delta_{e\mu} - |\eta_{e\tau}|s_{12}c_{12}s_{23}(1+s_{23}^2)\sin\delta_{e\tau} , \quad (\text{A7})$$

$$\Delta J_{e\mu}^{23} = \Delta J_{e\mu}^{31} = -\Delta J_{\mu\tau}^{12} = \Delta J_{\tau e}^{23} = \Delta J_{\tau e}^{31} . \quad (\text{A8})$$

-
- [1] P. Minkowski, Phys. Lett. **B67**, 421 (1977).
 - [2] T. Yanagida, in *Proc. Workshop on the Baryon Number of the Universe and Unified Theories*, edited by O. Sawada and A. Sugamoto (1979), p. 95.
 - [3] R. N. Mohapatra and G. Senjanović, Phys. Rev. Lett. **44**, 912 (1980).
 - [4] J. Schechter and J. W. F. Valle, Phys. Rev. **D22**, 2227 (1980).
 - [5] G. Lazarides, Q. Shafi, and C. Wetterich, Nucl. Phys. **B181**, 287 (1981).
 - [6] R. N. Mohapatra and G. Senjanović, Phys. Rev. **D23**, 165 (1981).
 - [7] R. Foot, H. Lew, X. G. He, and G. C. Joshi, Z. Phys. **C44**, 441 (1989).
 - [8] W. Buchmüller and C. Greub, Nucl. Phys. **B363**, 345 (1991).
 - [9] A. Pilaftsis, Z. Phys. **C55**, 275 (1992), hep-ph/9901206.
 - [10] G. Ingelman and J. Rathsman, Z. Phys. **C60**, 243 (1993).
 - [11] C. A. Heusch and P. Minkowski, Nucl. Phys. **B416**, 3 (1994).
 - [12] J. Kersten and A. Y. Smirnov, Phys. Rev. **D76**, 073005 (2007), arXiv:0705.3221.
 - [13] W. Chao, S. Luo, Z.-z. Xing, and S. Zhou, Phys. Rev. **D77**, 016001 (2008), arXiv:0709.1069.
 - [14] W. Chao, Z.-G. Si, Z.-z. Xing, and S. Zhou, Phys. Lett. **B666**, 451 (2008), arXiv:0804.1265.
 - [15] M. Malinský, T. Ohlsson, and H. Zhang, Phys. Rev. **D79**, 073009 (2009), arXiv:0903.1961.
 - [16] R. N. Mohapatra and J. W. F. Valle, Phys. Rev. **D34**, 1642 (1986).
 - [17] P. H. Frampton, S. L. Glashow, and T. Yanagida, Phys. Lett. **B548**, 119 (2002), hep-ph/0208157.
 - [18] W.-l. Guo, Z.-z. Xing, and S. Zhou, Int. J. Mod. Phys. **E16**, 1 (2007), hep-ph/0612033.
 - [19] P.-H. Gu, H. Zhang, and S. Zhou, Phys. Rev. **D74**, 076002 (2006), hep-ph/0606302.
 - [20] Z.-z. Xing (2007), arXiv:0706.0052.
 - [21] G. 't Hooft, C. Itzykson, A. Jaffe, H. Lehmann, P. Mitter, I. Singer, and R. Stora, eds., *Naturalness, chiral symmetry, and spontaneous chiral symmetry breaking* (1979).
 - [22] S. M. Bilenky and S. T. Petcov, Rev. Mod. Phys. **59**, 671 (1987).
 - [23] J. Schechter and J. W. F. Valle, Phys. Rev. **D25**, 774 (1982).
 - [24] S. Antusch, C. Biggio, E. Fernández-Martínez, M. B. Gavela, and J. López-Pavón, JHEP **10**, 084 (2006), hep-ph/0607020.
 - [25] F. Deppisch and J. W. F. Valle, Phys. Rev. **D72**, 036001 (2005), hep-ph/0406040.

- [26] A. Ilakovac and A. Pilaftsis, Nucl. Phys. **B437**, 491 (1995), hep-ph/9403398.
- [27] J. Bernabeu, A. Santamaria, J. Vidal, A. Mendez, and J. W. F. Valle, Phys. Lett. **B187**, 303 (1987).
- [28] F. del Aguila and J. A. Aguilar-Saavedra, Phys. Lett. **B672**, 158 (2009), arXiv:0809.2096.
- [29] G. Altarelli and D. Meloni, Nucl. Phys. **B809**, 158 (2009), arXiv:0809.1041.
- [30] T. Schwetz, M. Tórtola, and J. W. F. Valle, New J. Phys. **10**, 113011 (2008), arXiv:0808.2016.
- [31] S. Antusch, J. P. Baumann, and E. Fernández-Martínez, Nucl. Phys. **B810**, 369 (2009), arXiv:0807.1003.
- [32] A. Ibarra and G. G. Ross, Phys. Lett. **B591**, 285 (2004), hep-ph/0312138.
- [33] C. Jarlskog, Phys. Rev. Lett. **55**, 1039 (1985).
- [34] H. Fritzsch and Z.-z. Xing, Prog. Part. Nucl. Phys. **45**, 1 (2000), hep-ph/9912358.
- [35] H. Zhang and Z.-z. Xing, Eur. Phys. J. **C41**, 143 (2005), hep-ph/0411183.
- [36] T. Ohlsson and H. Zhang, Phys. Lett. **B671**, 99 (2009), arXiv:0809.4835.
- [37] D. Meloni, T. Ohlsson, and H. Zhang, JHEP **04**, 033 (2009), arXiv:0901.1784.
- [38] E. Fernández-Martínez, M. B. Gavela, J. López-Pavón, and O. Yasuda, Phys. Lett. **B649**, 427 (2007), hep-ph/0703098.
- [39] Z.-z. Xing, Phys. Lett. **B660**, 515 (2008), arXiv:0709.2220.
- [40] S. Goswami and T. Ota, Phys. Rev. **D78**, 033012 (2008), arXiv:0802.1434.
- [41] A. Donini, K.-i. Fuki, J. Lopez-Pavon, D. Meloni, and O. Yasuda, JHEP **08**, 041 (2009), arXiv:0812.3703.
- [42] M. Malinský, T. Ohlsson, and H. Zhang, Phys. Rev. **D79**, 011301(R) (2009), arXiv:0811.3346.
- [43] J. Tang and W. Winter (2009), arXiv:0903.3039.
- [44] M. Blennow and E. Fernández-Martínez (2009), arXiv:0903.3985.
- [45] S. Antusch, M. Blennow, E. Fernández-Martínez, and J. López-Pavón (2009), arXiv:0903.3986.
- [46] W. Rodejohann (2009), arXiv:0903.4590.
- [47] P. Huber, M. Lindner, and W. Winter, Comput. Phys. Commun. **167**, 195 (2005), hep-ph/0407333.
- [48] P. Huber, J. Kopp, M. Lindner, M. Rolinec, and W. Winter, Comput. Phys. Commun. **177**, 432 (2007), hep-ph/0701187.
- [49] D. Autiero et al., Eur. Phys. J. **C33**, 243 (2004), hep-ph/0305185.
- [50] P. Huber, M. Lindner, M. Rolinec, and W. Winter, Phys. Rev. **D74**, 073003 (2006), hep-

ph/0606119.

- [51] M. Malinský, J. C. Romao, and J. W. F. Valle, Phys. Rev. Lett. **95**, 161801 (2005), hep-ph/0506296.
- [52] S. Bertolini, L. Di Luzio, and M. Malinský, Phys. Rev. **D80**, 015013 (2009), arXiv:0903.4049.
- [53] F. Bazzocchi and S. Morisi (2008), arXiv:0811.0345.
- [54] M. Hirsch, S. Morisi, and J. W. F. Valle (2009), arXiv:0905.3056.